DAVID H. EGGLER *Geophysical Laboratory, 2801 Upton Street, Washington, D.C. 20008*
C. WAYNE BURNHAM *Department of Geosciences, Pennsylvania State University, University Park, Pennsylvania 16802*

Crystallization and Fractionation Trends in the System Andesite-H_2O-CO_2-O_2 at Pressures to 10 Kb

ABSTRACT

Phase relations of a Mount Hood andesite, which has the composition of an average orogenic andesite, have been determined as a function of O_2 fugacity at 1 atm and of H_2O fugacity to pressures of 10 kb, at O_2 fugacities of the quartz-fayalite-magnetite (QFM) buffer. All runs contained either a H_2O or H_2O–CO_2 fluid phase; melts in runs with a H_2O–CO_2 fluid phase were H_2O undersaturated. The H_2O contents of the melts and H_2O fugacities were calculated from $NaAlSi_3O_8$–H_2O thermodynamic data on the assumption of ideal mixing in the system H_2O–CO_2.

One-atmosphere runs show that melting relations of silicates are little affected by f_{O_2} but that both ilmenite- and magnetite-out temperatures are raised by higher f_{O_2}. Ilmenite precipitates at higher temperature than magnetite. In these runs and in all runs at high pressure with H_2O and H_2O–CO_2 fluid phases, oxides were not stable at temperatures of the silicate liquidus. Oxides might be stable on the silicate liquidus if f_{O_2} rose two or more log units above the Ni–NiO (NNO) buffer. However, calculations indicate that in natural magmas, those processes which might change f_{O_2}—crystal-liquid equilibria or exchange of H_2, or H_2 and H_2O with the wall rocks—cannot raise f_{O_2} by that magnitude. Because differentiation of basalt melts to andesite must involve iron-rich oxide phase subtraction, such fractionation models appear unreasonable.

For the Mount Hood andesite composition, plagioclase is the liquidus phase under H_2O–saturated conditions to 5 kb and under H_2O–undersaturated conditions at 10 kb when the H_2O content of the melt is less than 4.7 wt percent. For higher H_2O contents, either orthopyroxene or, at H_2O saturation at pressure greater than 8 kb, amphibole assumes the liquidus. In all cases, clinopyroxene crystallizes at lower temperature than orthopyroxene. Melting curves in the H_2O–undersaturated region may be contoured either as percent H_2O in melt or as $P_{e_{H_2O}}$; in either case, the topology of the various silicate melting curves is different from the case of H_2O–saturated melting. Therefore, melting relations determined at H_2O–saturated conditions cannot be used successfully to predict melting relations in the H_2O–undersaturated region.

Amphibole melting relations were studied isobarically at 5 kb as a function of temperature and fluid-phase composition. Amphibole has a maximum stability temperature of 940 ± 15°C for fluid compositions of 100 to 44 mole percent H_2O; for fluids containing more CO_2 than 56 percent (or, equivalently, less than 4.4 wt percent H_2O in melt), the melting temperature is lower. The same relations would be seen if CO_2 were not present and the melt were H_2O undersaturated. These rather low melting temperatures, relative to other silicate phases, preclude andesite generation by basalt fractionation involving amphibole at pressures less than 10 kb.

INTRODUCTION

Until the last few years, andesites have been regarded as the products of fractional crystallization of basaltic magma at crustal pressures. A particularly elegant model was proposed by Osborn (1959). More recent petrologic research has centered on mechanisms involving partial melting in the mantle, among them hydrous melting of basalt, leaving a residuum mainly of amphibole and aluminous

Geological Society of America Bulletin, v. 84, p. 2517–2532, 10 figs., August 1973

pyroxenes (Green and Ringwood, 1968; Holloway and Burnham, 1972), dry melting of quartz eclogite (Green and Ringwood, 1966), and hydrous melting of peridotite (Yoder, 1969; Kushiro, 1972).

To test the fractionation hypothesis and the reasonableness of hydrous conditions postulated by several other hypotheses, phase relations of an andesite from Mount Hood, Oregon, were determined under conditions of controlled temperature, total pressure, and fugacities of the volatile species H_2O, CO_2, H_2, and O_2. Owing to the difficulty of interpreting the results when all the above parameters are varied simultaneously, three separate experimental situations were investigated. First, temperature and f_{O_2} were varied at a total pressure of 1 atm, primarily to examine the stability of oxide phases in andesite melts. Second, phase relations of melts saturated with H_2O were studied from 1 to 10 kb, at f_{O_2}'s defined by the QFM buffer. Finally, melts undersaturated with H_2O were studied at the same total pressures and the same f_{O_2} buffer. H_2O undersaturation was achieved by diluting the fluid phase with CO_2.

WATER-SATURATED AND UNDERSATURATED MELTING

The maximum solubility of H_2O in andesite and basalt melts is a function primarily of pressure (Hamilton and others, 1964), and the amount of H_2O in a melt at any temperature and total pressure is directly related to the fugacity of H_2O in the system (Burnham and Davis, 1971). A melt saturated with H_2O coexists with a fluid phase consisting essentially of H_2O, because the mole fraction of dissolved silicates is negligibly small at crustal pressures. The f_{H_2O} in that melt, $f^m{}_{H_2O}$, equal to fugacity of H_2O in the fluid, $f^{fl}{}_{H_2O}$, is therefore only slightly less than the fugacity of pure water ($f^\circ{}_{H_2O}$) at the same temperature and total pressure. For practical purposes, then, H_2O saturation may be defined by the condition that $f^m{}_{H_2O} \approx f^\circ{}_{H_2O}$, whereas H_2O undersaturation is defined by the condition that $f^m{}_{H_2O} < f^\circ{}_{H_2O}$ at the same temperature and total pressure.

Although the condition of H_2O undersaturation is defined in terms of $f^m{}_{H_2O}$, we shall also use the terms $X^{fl}{}_{H_2O}$, the mole fraction of H_2O in a fluid phase, which is directly related to $f^m{}_{H_2O}$, and $P_{e_{H_2O}}$, which by definition is related to $f^m{}_{H_2O}$. The condition of H_2O undersaturation is also defined by $X^{fl}{}_{H_2O} < 1$ and $P_{e_{H_2O}} < P_{total}$.

When H_2O is the only volatile species, no fluid phase coexists with an H_2O–undersaturated melt. When a second volatile species exists which is insoluble in the melt, a fluid phase must *always* be present, and H_2O is partitioned between the melt and fluid, so that $f^m{}_{H_2O} = f^{fl}{}_{H_2O} < f^\circ{}_{H_2O}$.

Such a melt is always H_2O undersaturated by definition. CO_2 is essentially insoluble in granitic melts at low pressure (Wyllie and Tuttle, 1959), in basalt melt to 10 kb (Hill and Boettcher, 1970; Holloway and Burnham, 1972), and in albite melt to 30 kb (Millhollen and others, 1971). The position of a liquidus curve in P–T space, for a specific anhydrous bulk composition and f_{O_2}, depends upon $f^m{}_{H_2O}$, whether a H_2O CO_2 fluid or no fluid at all is present. Therefore, H_2O-undersaturated liquidus curves for a given amount of H_2O in the melt are the same in the system andesite–H_2O–CO_2 and in the system andesite–H_2O. Experiments by Eggler (1972a) have confirmed this reasoning.

The solidus is a somewhat different case. In the system andesite–H_2O, beginning of melting occurs at one of two univariant reactions (and, isobarically, at one of two temperatures), one in the presence of fluid and one in the fluid-absent region (Robertson and Wyllie, 1971). When CO_2 is added, these reactions become divariant, and melting occurs over a range of temperatures as a function of pressure and composition of the fluid (Holloway and Burnham, 1972).

EXPERIMENTAL TECHNIQUES

Rock Investigated

The rock studied from Mount Hood, Oregon, is a lava erupted in the late Pleistocene, after the bulk of Mount Hood was built (Wise, 1969). William S. Wise donated the sample, which was ground to <200 mesh in a mixer mill. Its analysis appears in Table 1.

A thin section of the rock contained plagioclase phenocrysts, one of which was analyzed (analysis 3, Table 1), and microphenocrysts of orthopyroxene and plagioclase set in a trachytic groundmass of plagioclase, orthopyroxene, clinopyroxene, glass, ilmenite, and magnetite. One glomerophenocryst (or xenocryst) of

plagioclase intergrown with orthopyroxene (analysis 2, Table 1) was found.

Water-Fugacity Control

Silicate-phase liquidi were determined under H_2O–saturated and undersaturated conditions from 0.5 to 8 kb in an internally heated pressure vessel (Burnham and others, 1969). The pressure medium was argon, and temperatures were read with three Chromel-Alumel or Pt-Pt10Rh thermocouples. Maximum errors for these runs are estimated at ±12°C and 0.35 kb but in most cases were less; error brackets in Figures 1 and 2 show estimated errors for each run, which are listed in Tables 2 and 3. A few runs were made at 10kb in a piston-cylinder apparatus, with errors as shown in Figure 2; techniques of Boettcher and Wyllie (1968) were used.

In H_2O–saturated runs, approximately 0.1 g of rock was loaded into a Pd50–Ag50 capsule with an excess of H_2O, and the capsule was welded shut. For H_2O-undersaturated runs, the oxalic acid technique (described at length by Eggler, 1972a) was used. A fluid phase was always present in the run, which promoted rapid achievement of equilibrium.

One mole of oxalic acid, loaded with rock into the capsule, initially produces 2 moles CO_2 and 2 moles H_2O at high temperature (Holloway and others, 1968), but H_2O must then be partitioned between melt and fluid. In the absence of thermodynamic data, it is assumed that H_2O mixes ideally in the fluid phase ($f^{fl}_{H_2O} = X^{fl}_{H_2O} \times f^{\circ}_{H_2O}$) and that CO_2 has negligible solubility in the melt. Because $f^{m}_{H_2O}$ can be related to $X^{m}_{H_2O}$ (the mole fraction of H_2O in melt) by the thermodynamic data of Burnham and Davis (1971) on melts in the $NaAlSi_3O_8$–H_2O system, the amount of oxalic acid to add to the capsule to achieve any amount of H_2O in the melt can be calculated (Eggler, 1972a).

When a large excess of oxalic acid is used, so that the amount of H_2O entering the melt is negligible compared to that in the fluid, percent H_2O in the melt is known no matter what the percent melt in the run, because the fluid contains 50 mole percent H_2O. Otherwise, the amount of glass must be known to calculate the amount of H_2O in the melt. Accordingly, modes of critical runs were counted in polished thin section. A few modes were calculated by a least-squares method from probe analyses of all phases (see Holloway and Burnham, 1972). Weight percents H_2O in the melt, listed in Table 3, are believed to be accurate to 0.5 percent.

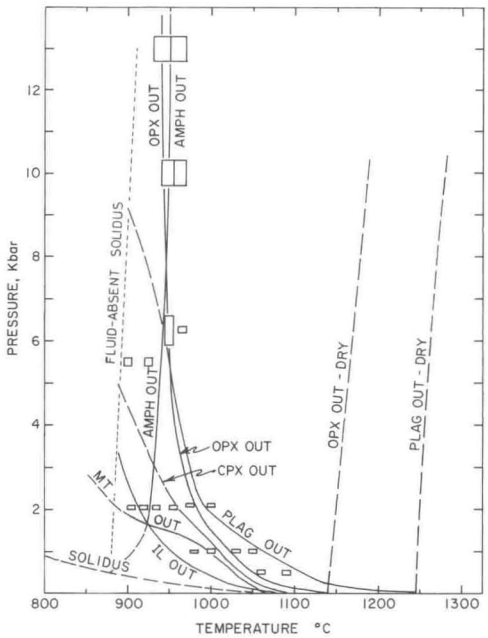

Figure 1. Phase relations for Mount Hood andesite composition at H_2O–saturated conditions at the QFM buffer. Runs at 10 and 13 kb from Allen and Boettcher (1971); dry liquidi extrapolated after Green and Ringwood (1968). Vapor-absent curve inferred.

Oxygen Buffering

The internally heated pressure vessel was fitted with a 60Pd–40Ag hydrogen membrane (Shaw, 1967) connected to a hydrogen tank and Heise gauge. P_{H_2} was maintained at a value to yield an oxygen fugacity, calculated from the $f^{m}_{H_2O}$ of the run, equal to that of the QFM buffer for the temperature and pressure of the run. The maximum relative error in hydrogen pressure was 6 percent. P_{H_2} in runs in the piston-cylinder was close to that of the NNO buffer for pure H_2O (Eggler, 1972a). Tables 2 and 3 list P_{H_2} and f_{O_2}.

Runs were made at 1 atm in 50Pd–50Ag envelopes in vertical quench furnaces wound with platinum and kanthal wire. Temperatures were controlled to ±3°C or less. Oxygen

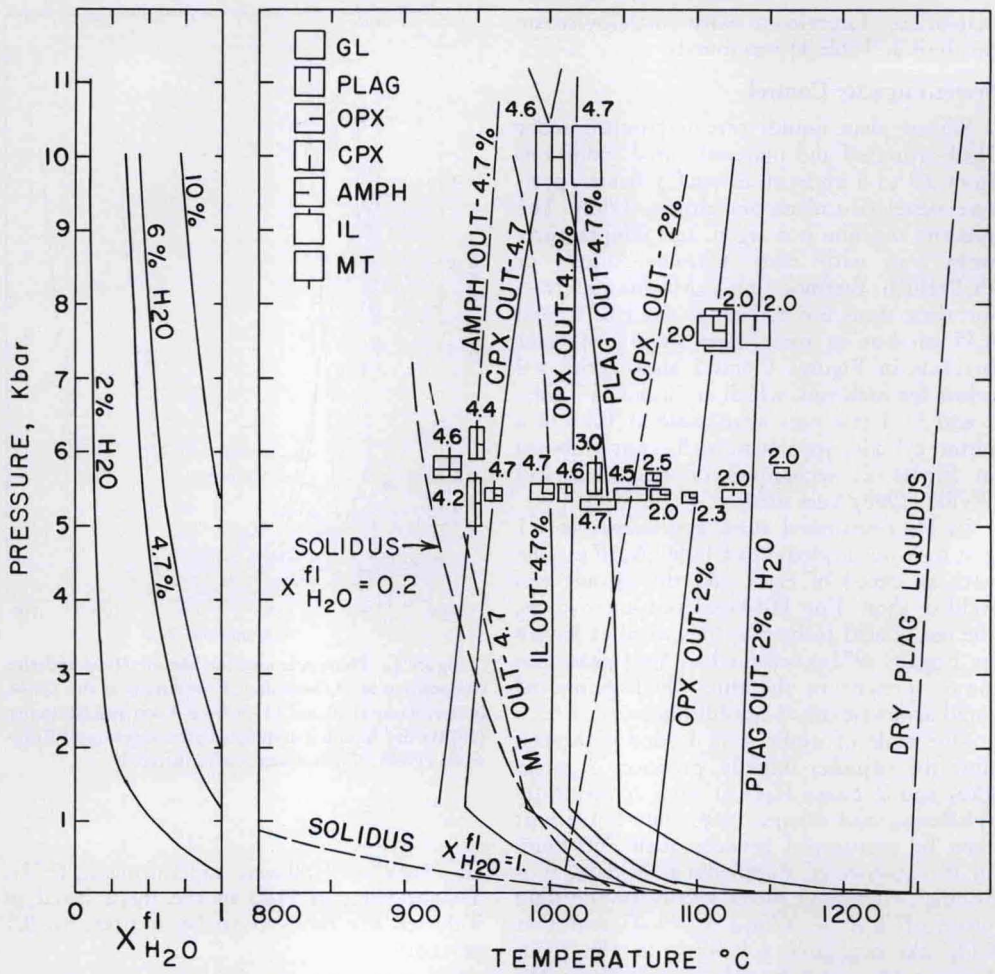

Figure 2. Phase relations at H_2O–undersaturated conditions. Numbers near run boxes indicate wt percent H_2O in melt of the run. Liquidi are drawn for H_2O contents in melt of 2.0 and 4.7 percent. Graph at left relates wt percent H_2O in melt to $X^{fl}_{H_2O}$ at 1,000° C.

fugacities were controlled by standard CO_2–H_2 gas-mixing techniques (Darken and Gurry, 1945). Both temperature and f_{O_2} were checked by determining the NNO reaction at 1,100° and 1,200°C.

Phase Identification and Analysis

All runs were crushed and examined in immersion oils. Opaque phases were identified in polished section under oil and magnified ×1,500. Probe analyses were performed on ARL–AMX and EMX instruments by techniques described previously (Eggler, 1972a).

EXPERIMENTAL RESULTS

Phase Relations

Runs at 1 atm appear in f_{O_2}–T projection in Figure 3. While silicate liquidi are apparently little affected by f_{O_2}, stability of the oxides, ilmenite and magnetite, is increased by higher f_{O_2}. Ilmenite is a rhombohedral phase which is a solid solution of ilmenite ($FeTiO_3$) and hematite (Fe_2O_3). Magnetite is a spinel phase which is a solid solution of magnetite (Fe_3O_4) and ulvospinel (Fe_2TiO_4). Perhaps surprisingly, ilmenite crystallizes at a higher temperature

TABLE 1. COMPOSITIONS OF PHASES AND BULK ROCK

Analysis	1	2	3	4	5	6	7
phase	bulk	opx	plag	opx	opx	opx	opx
P(bars)	rock	(phenocrysts in		1,000	5,620	5,430	10,000
T(°C)		natural rock)		980	1,070	1,010	1,000
wt % H_2O in melt				4.3	2.5	4.6	4.6
SiO_2	59.1	54.7	54.4	51.4	52.3	52.4	51.0
TiO_2	0.94	0.31	0.05	0.50	0.34	0.33	0.41
Al_2O_3	17.8	1.45	28.8	0.79	1.60	1.99	1.09
FeO*	6.43	18.2	0.22	22.5	21.0	19.4	22.3
MgO	3.05	24.7	0.00	22.5	22.6	24.2	21.5
CaO	6.85	1.35	11.9	1.75	1.42	1.51	1.67
Na_2O	4.27	0.07	4.8	n.d.	0.09	n.d.	0.05
K_2O	1.08	0.01	0.18	n.d.	0.09	n.d.	0.01
Total	99.52	100.79	100.35	99.44	99.44	99.83	98.03

*Total Fe as FeO. Opx = Orthopyroxene, plag = Plagioclase.

than magnetite. In the f_{O_2}–T range we consider reasonable for natural conditions, between the dotted lines on Figure 3, magnetite and ilmenite crystallize 20° to 45°C below the orthopyroxene liquidus and well below the plagioclase liquidus.

Phase relations at H_2O–saturated conditions at the QFM buffer appear in P–T projection in Figure 1 and at H_2O–undersaturated conditions in Figure 2. Figure 2 also shows the relation between weight percent H_2O in the liquid and $X^{fl}_{H_2O}$, as discussed by Eggler (1972a). Water-undersaturated liquidi for anhydrous phases are drawn for H_2O contents in melts of 2.0 and 4.7 percent H_2O. Melting curves for orthopyroxene and plagioclase do not have the same slope because of differences in the ΔV_r and ΔS_r of the melting reactions. The curves are nearly linear at low H_2O contents and become steeper, relative to the dry liquidi, with increasing H_2O content.

Phase relations are clarified by calculation of a T–X section from Figures 1 and 2. Figure 4 clearly shows the melting relations as a function of H_2O content and $X^{fl}_{H_2O}$ at 5 kb total pressure. In the calculation we assume melting temperatures with pure CO_2 are those of the dry liquidi. The diagram also contrasts melting of Mount Hood andesite with a Paricutin andesite (Eggler, 1972a). Liquidi slopes are similar for the two rocks, but their relative positions are different. For example, plagioclase is the liquidus phase in the Mount Hood andesite for all H_2O contents, while orthopyroxene assumes the liquidus in the Paricutin andesite at about 2 percent H_2O.

Oxides are also stable to higher temperature in the Mount Hood andesite. As at 1 atm, ilmenite appears first, but the relation between ilmenite and magnetite is not entirely clear, inasmuch as in 1 kb H_2O–saturated runs, magnetite appears with ilmenite, but at 2 kb, magnetite crystallizes at least 60°C below ilmenite. H_2O–undersaturated runs indicate that at the QFM buffer, ilmenite appears at least 35°C below the silicate liquidus and magnetite becomes unstable relative to ilmenite with increasing pressure.

The upper temperature limit of amphibole stability is 950°C at 12 kb and H_2O–saturated conditions (Allen and Boettcher, 1971; Fig. 1). Recent investigations (Hill and Boettcher, 1970; Holloway and Burnham, 1972; Holloway, 1973; Eggler, 1972b) have shown that under H_2O–undersaturated conditions the upper temperature limit of amphibole stability may either increase or decrease relative to the H_2O–saturated stability curve. In the pressure range to 10 kb, however, the amphibole-out curve will lie within 20°C of the H_2O–saturated curve unless the melt contains less than about 3.5 wt percent H_2O. Runs on Mount Hood andesite at 5.5 kb containing 4.0 to 4.7 percent H_2O show that amphibole is as stable, within experimental limits, as when the melt is H_2O saturated (10 percent H_2O). However, under

TABLE 2. RESULTS OF EXPERIMENTAL RUNS AT H_2O–SATURATED CONDITIONS

Conditions of run						Phases present*
P(Kb)	T,°C	P_{H_2} (b)	Time (hrs)	-log f_{O_2} (b)	Initial (%H_2O)	
0.50	1,090	8.6	5.5	9.69	3.4	gl, pl
0.50	1,060	8.6	17.5	10.13	5.0	gl, pl
1.00	1,050	18.1	23	10.35	10.5	gl, pl
1.00	1,030	18.1	23	10.66	6.6	gl, pl, opx(tr.)
1.02	1,000	7.0	28	10.28	6.0	gl, pl, opx, il, mt(sa)
1.00	980	7.4	36	10.68	6.7	gl, pl, opx, il, mt
2.12	1,000	30.0	27	10.92	8.7	gl
2.12	975	30.0	27	11.34	7.8	gl, pl(sa), opx(tr.)
2.04	955	28.6	21	11.68	7.5	gl, pl, opx, il
2.04	935	28.6	21	12.04	8.3	gl, pl, opx, il
2.07	925	28.6	24	12.21	10.8	gl, opx, pl, hb, il
2.07	905	28.6	24	12.59	10.4	gl, opx, cpx(sa), pl, hb, il
5.52	925	78.0	12	12.06	15.7	gl, hb, opx(sa), pl
5.52	900	78.0	12	12.54	13.7	gl, hb, opx, pl
6.27	965	98.7	2.25	11.37	14.5	gl
6.27	950	66.2	20	11.29	13.2	gl, opx(sa), pl(tr.)

*gl = glass, pl = plagioclase, opx = orthopyroxene, cpx = clinopyroxene, il = ilmenite-hematite solid solution, mt = magnetite-ulvospinel solid solution, tr. = trace, sa = small amount.

H_2O–undersaturated conditions, amphibole is never stable at temperatures near the plagioclase liquidus.

Phase Compositions

Orthopyroxenes encountered in run products are moderately aluminous (Table 4); in some cases, certain grains inverted upon quenching to a clinopyroxene which had a small extinction angle. No plagioclase, amphibole, or clinopyroxene could be analyzed from run products. Amphiboles should be similar to tschermakitic hornblendes from Paricutin andesite runs (Eggler, 1972b) and clinopyroxenes should be similar to those in Paricutin runs, which contained 42 mole percent wollastonite and a maximum of 4.4 percent Al_2O_3 at 10 kb.

OXIDE FRACTIONATION IN THE CALC-ALKALINE SUITE

Various geochemical arguments regarding the fractional crystallization hypothesis of andesite origin have been reviewed by Green and Ringwood (1968). Phase equilibria questions revolve about the problem of iron oxide stability. Model system studies (Osborn, 1959; Roeder and Osborn, 1966; Eggler and Osborn, 1969) and mass-balance calculations

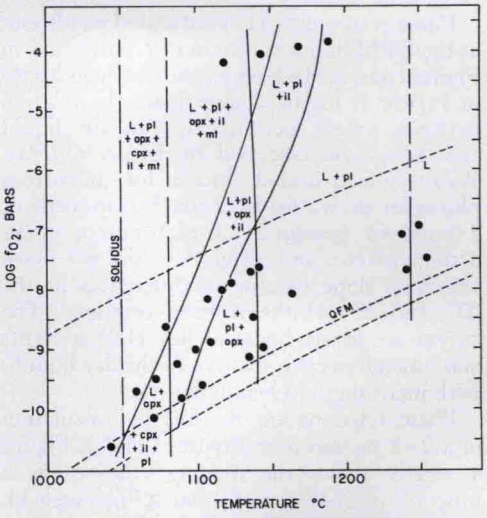

Figure 3. Phase relations for Mt. Hood andesite as a function of F_{O_2} at 1 atm total pressure. Stability limits are long dashed where approximately located. Short dashes contain region of f_{O_2} values expected in natural magmas.

show that magnetite must be subtracted from a basalt melt, along with silicates, to yield an andesite melt derivative. An iron-rich oxide phase must therefore be stable in a parent basalt melt, each succeeding melt, and the

TABLE 3. RESULTS OF EXPERIMENTAL RUNS AT H_2O–UNDERSATURATED CONDITIONS

Conditions of run									Phases present†
P (kb)	T (°C)	P_{H_2} (b)	Time (hrs)	Oxalic acid (wt %)	Est. % glass (wt)	H_2O in melt (wt %)	m f_{H_2O} (b)	-log f_{O_2} (b)	
5.75	1,158	18.0	4	7.3	100	2.0	987	8.83	gl
5.43	1,125	19.5	10	7.7	99.8	2.0	891	9.41	gl, pl(tr.)
5.40	1,095	18.4	14	7.7	80	2.3	1,121	9.57	gl, pl, opx(sa)
5.62	1,070	26.2	25	7.7	74.5*	2.5	1,340	10.08	gl, pl, opx
5.45	1,070	46.8	22	30.6	100	4.3	2,657	9.99	gl
5.45	1,075	10.0	21	5.7	71.6*	2.0	882	9.53	gl, pl, opx
5.43	1,055	49.1	7	40.0	100	4.5	2,753	10.22	gl
5.30	1,034	49.1	12.5	47.3	93	4.7	2,790	10.52	gl, pl
5.43	1,010	40.7	30	41.2	85	4.6	2,770	10.73	gl, pl, opx(sa)
5.65	1,030	10.5	23	5.7	36.4*	3.0	1,720	9.66	gl, opx, pl, cpx(sa), il
5.47	995	42.0	24	35.9	70	4.7	2,844	10.98	gl, opx, pl, il
5.43	970	17.8	24	5.5	20.1*	3.7	2,033	12.38	gl, opx, pl, il, cpx(sa)
5.41	960	43.8	22.5	33.6	60	4.7	2,735	11.63	gl, opx, cpx(tr.), pl, il
5.31	968	27.6	24	9.3	30	4.0	2,200	11.28	gl, opx, cpx, pl, il
6.12	950	40.0	24	20.0	38.7*	4.4	2,906	11.67	gl, opx, cpx(sa), pl, il
5.31	948	27.6	24	8.7	19.5*	4.2	2,313	11.58	gl, opx, cpx, pl, mt, il
5.80	930	51.0	25	33.4	60	4.6	2,910	12.23	gl, cpx, opx, pl, il, hb
7.65	1,140	22.7	6	7.4	99.5	2.0	1,340	9.00	gl, pl(sa)
7.65	1,115	22.7	6	7.3	97	2.0	1,331	9.33	gl, pl
7.65	1,110	22.7	6	7.5	95	2.0	1,331	9.40	gl, pl, opx(sa)
10.0	1,025	86.6	7	26.2	100	4.7	6,100	10.48	gl
10.0	1,000	86.1	6	24.0	95	4.6	5,970	10.88	gl, cpx, opx, pl(sa)

**Percent glass determined by point count, or from calculated mode.*
†gl = glass, pl = plagioclase, opx = orthopyroxene, cpx = clinopyroxene, il = ilmenite-hematite solid solution, mt = magnetite-ulvospinel solid solution, tr. = trace, sa = small amount.

final andesite melt, because a phase, once in equilibrium with a melt, cannot disappear except by reaction or by the placement of the melt, once separated, in a different regime of intensive parameters. Osborn (1969) has argued the latter case, that magnetite would be more stable at high pressure than at low and therefore could be important at high pressure in deriving an andesite melt but absent in a lava erupted at low pressure. Such a lack of magnetite in andesite is common (Carmichael and Nicholls, 1967). A model system at high pressure (Eggler, 1971) and the present study provide no evidence of a pressure effect on magnetite stability.

Role of Oxide Phases

For the Mount Hood andesite composition, the iron-oxide phase first appearing is ilmenite, not magnetite, as in the model systems. In a mass-balance calculation designed to produce average andesite from tholeiite by subtraction of olivine, clinopyroxene, plagioclase, and iron-titanium oxide, the substitution of ilmenite for magnetite is of little consequence, for only 2 to 2.5 wt percent oxide need be subtracted, and either ilmenite or titaniferous magnetite serves equally well. However, the fractionation model typified by the systems FeO–Fe_2O_3–SiO_2–MgO (Osborn, 1959) and CaO–MgO–FeO–Fe_2O_3–SiO_2 (Presnall, 1966) is critically dependent on the presence of magnetite, rather than ilmenite. The crucial step in obtaining a silica-enrichment trend and suppressing an iron-enrichment trend is maintenance of the Fe_2O_3/FeO ratio of the melt, by external buffering of f_{O_2}, even as precipitation of magnetite threatens to lower that ratio. A lower Fe_2O_3/FeO ratio allows fractionating liquids to crystallize more Mg-, Fe-rich silicates, subtraction of which lowers the Mg/Fe ratio of the liquid. These relations

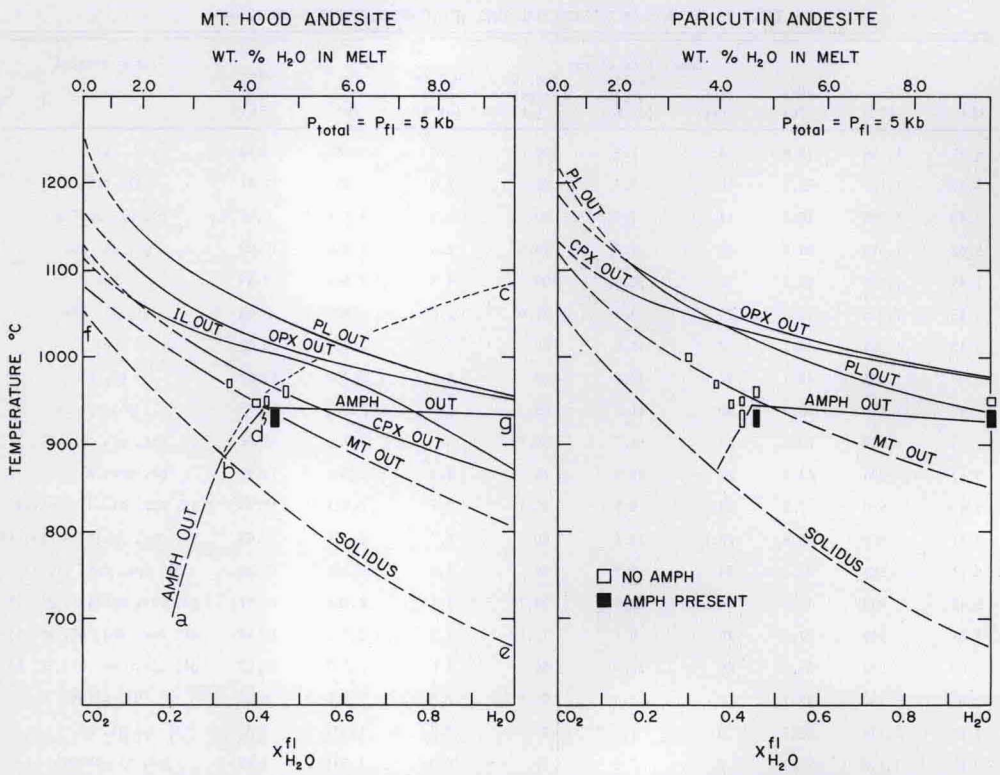

Figure 4. *T-X* **sections at 5 kb for Mount Hood andesite and Paricutin andesite (Eggler, 1972a). Liquidi dashed where approximately located; run boxes show experimental determination of amphibole stability. Amphibole dehydration curve (abc) inferred; short dashed where metastable.**

hold precisely because magnetite has a higher Fe_2O_3/FeO ratio than silicate melt; f_{O_2} buffering maintains the magnetite stability field. Precipitation of ilmenite with a low Fe_2O_3/FeO ratio would change the phase relations entirely.

Furthermore, melting studies of basalts (Holloway and Burnham, 1972; Yoder and Tilley, 1962) show magnetite or magnesioferrite, not ilmenite, as the nearer liquidus phase. If basalts are the fractionation parents of andesites, it is curious that a typical andesite contains ilmenite as the highest melting oxide phase.

Most important, we note that neither ilmenite nor magnetite is stable near the silicate liquidus at any of the conditions investigated (Figs. 1, 2, and 3) and thus could not have played a role in fractionation. There is, of course, a possibility that higher f_{O_2}, possibly combined with depression of the plagioclase liquidus by a few percent H_2O, could produce suitable conditions for Fe-Ti oxide stability at the liquidus. The following sections examine that possibility.

Magnitude of Oxygen Fugacities

Perhaps the most reliable indicator of oxygen fugacity in natural magmas is the composition of coexisting magnetite-ilmenite pairs (Buddington and Lindsley, 1964). Some values obtained from this geobarometer-thermometer on basalts and calcalkaline rocks are presented in Figure 5, including one from the andesite studied. Unfortunately, many of these values probably do not represent near-liquidus conditions. We shall argue below, however, that f_{O_2} varies in a melt-crystal system along lines subparallel to the buffers shown, so that the range of f_{O_2} in subalkaline and calcalkaline systems lies between the dashed lines. It appears that at higher, magmatic temperatures, f_{O_2} values are below NNO.

A second f_{O_2} indicator, comparison of the Fe_2O_3/FeO ratio of a rock with Fe_2O_3/FeO ratios of experimentally produced melts, is

TABLE 4. RESULTS OF EXPERIMENTAL RUNS AT 1 ATM

Conditions of run			Phases present*
T (°C)	$-\log f_{O_2}$ (bars)	time (hrs)	
1,255	7.48	31	gl
1,250	6.94	24.5	gl
1,241	7.68	65	gl, pl
1,238	7.08	24.5	gl, pl(tr.)
1,189	3.84	41	gl, pl
1,169	3.93	50	gl, pl, il
1,164	8.08	48	gl, pl
1,144	4.05	30.5	gl, pl, il, mt(sa)
1,144	8.99	61	gl, pl
1,142	7.62	52	gl, pl
1,137	8.48	49.5	gl, pl, opx
1,136	7.70	48.5	gl, pl, opx(tr.)
1,134	9.13	58	gl, pl, opx
1,123	7.90	48	gl, pl, opx
1,120	4.19	34.3	gl, pl, opx, il, mt
1,117	8.01	49	gl, pl, opx, il(tr.)
1,109	8.90	55	gl, pl, opx
1,107	8.17	50	gl, pl, opx, il
1,103	9.60	59.5	gl, pl, opx
1,099	9.02	64.5	gl, pl, opx, il(tr.)
1,090	9.81	73	gl, pl, opx, il(sa)
1,086	9.26	68	gl, pl, opx, il
1,079	8.63	53	gl, pl, opx, cpx(sa), il, mt(sa)
1,072	9.49	55.5	gl, pl, opx, il, cpx(sa)
1,070	10.13	102	gl, pl, opx, il, cpx
1,059	9.70	60.5	gl, pl, opx, cpx, mt, il
1,042	10.60	105	pl, opx, cpx, il, mt

*gl = glass, pl = plagioclase, opx = orthopyroxene, cpx = clinopyroxene, il = ilmenite-hematite solid solution, mt = magnetite-ulvospinel solid solution, tr. = trace, sa = small amount.

judged to be of lesser value. Volcanic rocks are known to be oxidized by subsolidus reactions with gases; even ignoring that problem, the relation of the Fe_2O_3/FeO ratio of a rock, which is a subsolidus ratio or a hypersolidus ratio quenched from an unknown temperature, to a ratio at an assumed liquidus, is not clear. Nevertheless, the range of values deduced by Fudali (1965) for some basalts and andesites (Fig. 5) is within our limits.

Control of Oxygen Fugacity

It is also of interest to evaluate the controls of f_{O_2} in magmatic processes, and in turn to evaluate the relation of values of Figure 5 to values at higher liquidus temperatures and the extent to which f_{O_2} may vary during fractional crystallization. Various aspects of this subject have been discussed by Carmichael and Nicholls (1967), Anderson (1968), Mueller (1969, 1971), Osborn (1969), and Hamilton and Anderson (1967) among others.

As pointed out by Mueller (1969), two reactions are important in controlling f_{O_2} of a melt, the oxidation of FeO to Fe_2O_3, and the H_2O gas reaction. These may be combined in one equilibrium constant:

$$K = (a_{FeO_{1.5}}/a_{FeO})^2 (f_{H_2}/f_{H_2O}) . \quad (1)$$

Whether the first ratio or the second controls f_{O_2} of the melt is simply a question of which is the larger O_2 reservoir. Mueller (1969) and Hamilton and Anderson (1967) argue that in closed systems the second term is the more important when "significant" amounts (probably more than one percent) of H_2O are present. In open systems, the $FeO_{1.5}/FeO$ ratio of the magma is even more likely merely to reflect, rather than control, f_{O_2}.

Now consider four cases of f_{O_2} variation in a system whose components are an anhydrous rock composition and one or more volatile species; two cases involve a magma system closed and two involve a system open to the wall rocks.

1. The system is closed, and the melt contains a negligible amount of H_2O. In this case, f_{O_2} is controlled by the ratio ($FeO_{1.5}$/FeO), which has been considered for a melt without crystals by Anderson (1968). He found a slope ($d \log f_{O_2}/d(1/T)$) $= -3.0 \times 10^4$ reasonable. Such a curve for an arbitrary ($FeO_{1.5}$/FeO) ratio is plotted in Figure 6. If crystal-liquid equilibria are not considered, fractionation along such a curve would lower f_{O_2} relative to the QFM buffer. The effects of crystallization of ferromagnesian silicates and oxides on the ($FeO_{1.5}$/FeO) ratio has been considered in model systems such as MgO–FeO–Fe_2O_3–SiO_2 (Osborn, 1959). Closed-system fractionation by silicate removal may initially raise ($FeO_{1.5}$/FeO) and, accordingly, raise f_{O_2}, relative to the curve shown, but eventually, subtraction of magnetite will lower ($FeO_{1.5}$/FeO) and lower f_{O_2}, as discussed above. Subtraction of an iron-rich phase is needed (somewhat paradoxically) to produce the iron-enrichment trend.

2. The system is closed, but f_{O_2} is controlled

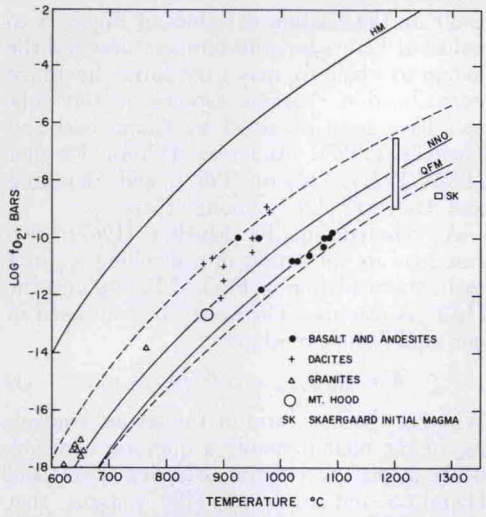

Figure 5. Estimates of f_{O_2} and temperature in basaltic and calcalkaline magmas. Dotted lines identical to lines in Figure 3. Data from Carmichael (1967), Carmichael and Nicholls (1967), Buddington and Lindsley (1964), and Williams (1971). Bar at 1,200°C from Fudali (1965).

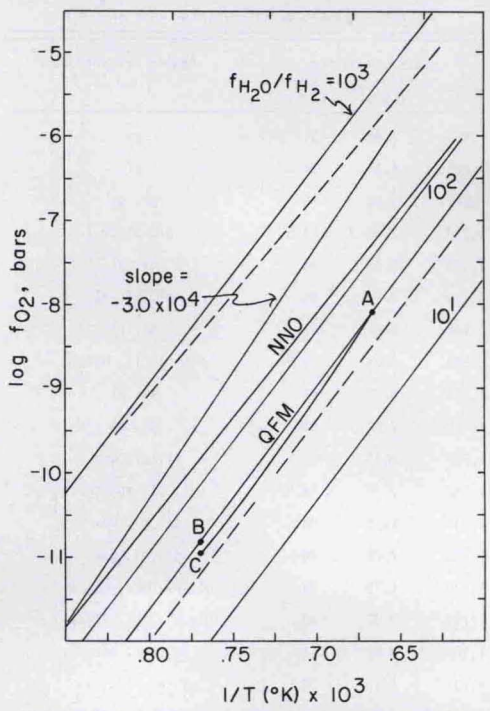

Figure 6. Equilibrium f_{O_2} for various f_{H_2O}/f_{H_2} ratios as a function of temperature. Dotted lines identical to estimate of natural range of f_{O_2} in Figure 3.

by the ratio (f_{H_2O}/f_{H_2}). H_2O may be dissolved in the melt and may also be present in a fluid consisting of H_2O or H_2O and CO_2. Figure 6 contains contours of (f_{H_2O}/f_{H_2}), calculated from thermodynamic data (K_W) of Robie and Waldbaum (1968). Because f_{H_2O} and f_{H_2} in a fractionating magma change with temperature and total pressure, we continue to make the simplifying assumption of ideal mixing of the gases, in order to calculate f_{O_2} changes.

To illustrate, consider a H_2O–saturated magma initially at the QFM buffer at 1,227° C and 5 kb total pressure. We use the assumption of ideal mixing and the definition of partial pressure:

$$f^{fl}_{H_2O}/f^{\circ}_{H_2O} = X^{fl}_{H_2O} \equiv P_{H_2O}/P_{total} \quad (2)$$

$$f^{fl}_{H_2}/f^{\circ}_{H_2} = X^{fl}_{H_2} \equiv P_{H_2}/P_{total} \quad (3)$$

It should be noted that pressures are *partial* pressures, in accordance with assumptions of ideal mixing, rather than P_{eH_2O} used elsewhere in this paper.

At 1,227°C, the ratio ($f^{fl}_{H_2O}/f^{fl}_{H_2}$) is defined by K_W and f_{O_2}. Because $f^{\circ}_{H_2}$ and $f^{\circ}_{H_2O}$ can be obtained from tables (Shaw and Wones, 1964; Holloway and others, 1971), equations (2) and (3) may be solved simultaneously to obtain $X^{fl}_{H_2O}$ and $X^{fl}_{H_2}$, remembering that $X^{fl}_{H_2O} + X^{fl}_{H_2} = 1$. Now, those mole fractions, known at one temperature in the system, remain constant at another temperature if the gases mix ideally ($[\delta \ln a_i/\delta T]_{x_j} = [\delta \ln x_i/\delta T]_{x_j} = 0$); therefore values of $f^{fl}_{H_2O}$ and $f^{fl}_{H_2}$ at any other temperature can be calculated and, from those fugacities and K_W, f_{O_2}. Two cases are presented in Figure 6, A–B, a trend along which a magma cools from 1,227°C to 1,027°C at a total pressure of 5 kb, and A–C, a trend along which a magma cools from 1,227°C to 1,027°C while total pressure drops from 5 kb to 1 kb. Trend A–B is identical to the QFM trend, and A–C nearly parallels QFM. The trend of a differentiating H_2O–undersaturated magma should also nearly parallel QFM, for if a reservoir of H_2O and CO_2 is present, we may write that

$$P_{H_2} + P_{H_2O} = P_{total} - P_{CO_2}; \quad (4)$$

this case is then analogous to those discussed above, inasmuch as the right-hand term is constant at constant pressure. Therefore, f_{O_2} will follow one of the trend lines. If no CO_2 is present, and H_2O is present only in solution in melt, both f_{H_2O} and f_{H_2} will increase as

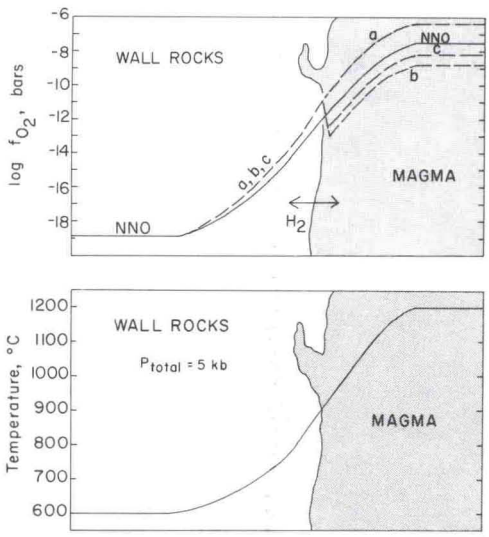

Figure 7. Oxygen fugacities produced in a magma by exchange of H_2 with wall rocks. Trends a, b, and c refer to case 3 in text.

anhydrous phases crystallize, probably in a nearly constant ratio, again resulting in a trend parallel to one of the lines shown.

3. The system is open, but the magma exchanges only H_2 with the wall rocks. Assuming H_2 can diffuse with ease, this case is likely in two instances: one, when H_2O is the only volatile species and there is no fluid phase. To exchange with wall rocks, H_2O must diffuse through the magma, a very slow process (Burnham, 1967). In the second instance, a fluid phase exists but has no passage to the wall rocks because of an impenetrable barrier, perhaps a rind of solidified magma.

Calculation of f_{O_2} is simplified by use of a model in which P_{total} = 5 kb, magma temperature is constant at 1,200°C, except at its margins, wall rocks are at 600°C, and the magma–wall-rock contact is at 900°C. In the wall-rock reservoir, $P_{H_2O} + P_{H_2} + P_{CO_2} = P_{total}$, and the solid Fe-bearing phases of the wall rocks control f_{O_2} of the entire system, wall rocks plus magma. Two typical wall-rock assemblages are biotite–K-feldspar–magnetite (+ quartz) and orthopyroxene-quartz-magnetite; the f_{O_2} buffering reactions are the oxidation-dehydration of annite to K-feldspar and magnetite, and the oxidation of ferrosilite to magnetite and quartz. Data on natural biotites indicate that they buffer f_{O_2} near NNO (Dodge and others, 1969). Calculation of the $FeSiO_3$ reaction from thermochemical data of Williams (1971), assuming $X_{FeSiO_3} = 0.2$ and $X_{Fe_3O_4} = 0.4$ in natural assemblages, yields f_{O_2} within 0.2 log units of NNO at 600°C. Such buffers then define the f_{H_2O}/f_{H_2} ratio of the wall rocks.

Three examples, which span a reasonable range of geologic conditions, illustrate the calculations:

a. Consider that in the magma and wall rocks the only volatile species are H_2O and H_2. If the wall rocks contain an assemblage such as biotite–K-feldspar–magnetite, their f_{O_2} is near NNO, which at 600°C controls log $f_{O_2} = -18.92$ and P_{H_2} = 9.8 b. In wall rocks at the contact at 900°C, log $f_{O_2} = -10.91$. That value is calculated by the same method outlined in section 2, assuming H_2O and H_2 exchange throughout the wall-rock reservoir. As Figure 7 shows, wall rocks are locally oxidized, relative to NNO, near the contact. Because f_{H_2} is equal in wall rocks and magma at the contact, and because f_{H_2O} is nearly equal in the magma at the contact at 900°C log $f_{O_2} = -10.91$, a value 0.9 log units greater than the NNO buffer. In the magma at 1,200°C, log $f_{O_2} = -6.20$, a value 1.3 log units greater than NNO (Fig. 7).

b. Consider that in the wall rocks $P_{H_2O} + P_{H_2} = P_{total}$, but that the magma contains 1 wt percent H_2O ($f^m_{H_2O}$ = 290 bars at 1,200°C). Because the assumption of ideal mixing certainly does not hold in melts, we shall also require that a fluid phase exist in equilibrium with the magma. Again in the wall rocks at the contact log $f_{O_2} = -10.91$ and f_{H_2} = 9.8 b. In the magma at the contact f_{H_2} = 9.8 b and, because $_{H_2}$ behaves nearly ideally, P_{H_2} = 9.8 b. From formula (3) we can then calculate that at 900°C, $X^{fl}_{H_2} = 0.002$. At 1,200°C, $X^{fl}_{H_2O} = 290/5{,}948 = 0.048$. Those mole fractions hold throughout the magma, provided the fluid moves freely. Therefore $X^{fl}_{CO_2}$, at any temperature in the magma, equals 0.95. In the magma near the contact at 900°C, $f^{fl}_{H_2O} = 0.048 \times 5{,}118 = 245$ b. Log f_{O_2} therefore is −13.55, considerably less than in wall rocks across the assumed barrier (see Fig. 7). Because we know the fugacities of H_2O and H_2 (9.8 b) at 1,200°C, we calculate that at 1,200°C, log $f_{O_2} = -8.82$, 1.3 log units less than NNO. If the magma were to cool from that temperature, $f^m_{H_2O}$ would increase, because of the subtraction of anhydrous phases, and f_{O_2} would, in relation to NNO, increase. The increase would

be slight, for if magma temperature fell to 1,100°C and the H_2O content doubled, probably an unrealistically high increase, then $f^m_{H_2O}$ = 827 bars; because P_{H_2} continues to be 9.8 b, log f_{O_2} = −9.18, 0.4 log units below NNO.

c. If the wall rocks contain an impure pore fluid, such that $f_{H_2O} = 0.5 \times f^\circ_{H_2O}$, and are buffered at NNO, log f_{O_2} again is −18.92 at 600°C, but f_{H_2} = 4.9. By reasoning analogous to case b, if the magma contains 1 percent H_2O, log f_{O_2} in the magma is −8.22 at 1,200°C, 0.7 log units less than the NNO buffer.

In summary, H_2 diffusion through a magma and equilibration with fluid in cooler wall rocks will control f_{O_2} within 1.3 log units of the wall-rock buffer curve under a variety of geologic conditions except, as we note below, at shallow depths. In the most probable cases, such as b and c, in which the magma contains only 1 or 2 percent of H_2O, f_{O_2} is *lowered* in the magma. In any case, f_{O_2} should fall in the range between the dotted lines on Figure 6. Differentiation of a magma would proceed generally along a path with a slightly shallower slope than the wall-rock buffer curve, but would depend somewhat on initial and final H_2O contents of the magma.

4. The system is open, and the magma exchanges H_2O *and* H_2 with wall rocks. If exchange is complete, f_{O_2} values must lie on a curve such as A–B (Fig. 6), as calculated in example 2. If exchange is incomplete, then f_{H_2O} in the magma near the contact generally is less than f_{H_2O} in the wall rocks near the contact (unless fluid in the wall rocks is very impure). In that case, f_{O_2} in the magma is less than that defined by a curve parallel to A–B (as in case 3b). If both H_2O and CO_2 are exchanged, the same types of situations apply, but f_{O_2} values will be slightly higher, analogous to case 3c.

Case 4 illustrates that H_2O which may enter a magma need *not* be oxidizing if it is in equilibrium with silicate-oxide assemblages. In the usual case of H_2O diffusion into a melt, f_{O_2} is lowered, relative to some buffer, rather than raised.

Summary

We have shown that in a variety of geologically possible situations, f_{O_2} in a magma within the crust is controlled largely by the initial $FeO_{1.5}/FeO$ or f_{H_2O}/f_{H_2} ratio of the magma or by the f_{O_2} buffering assemblage of the wall rocks. Differentiation of the magma or exchange of fluid with wall rocks will move f_{O_2} no more than 1.3 log units from the original buffer. Various geobarometers indicate that initial f_{O_2} values in magmas and f_{O_2} values in normal wall-rock assemblages are near NNO. Only unusual conditions can move f_{O_2} in a magma very far away from that buffer.

Unusual conditions may be encountered near the roofs of shallow magma chambers. Because waters are more oxidized at higher levels, either by meteoric water influx or by equilibration with oxidized sediments, exchange of H_2O or H_2 would oxidize the magma. Exchange of H_2O would also be facilitated by extensive fracture development, a common feature of chamber roofs. Extensive fractionation of a magma does not take place at such depths, however, but rather at deeper levels under conditions specified above.

We have previously shown that iron-titanium oxide phases are not stable at temperatures of silicate liquidi in andesite melt, under a variety of conditions, when f_{O_2} values are near NNO. We have also argued that to produce andesite by fractional crystallization of basalt, iron-titanium oxide must precipitate with the silicates. This basic inconsistency raises very serious questions about the fractional crystallization hypothesis.

WATER-UNDERSATURATED MELTING IN CALC-ALKALINE MELTS

Melting relations in the system andesite–H_2O–CO_2 are a guide to melting behavior in the H_2O–undersaturated region of most calc-alkaline melts, especially to behavior in the presence of a complex fluid phase. Figure 4 contains T–X sections showing melting relations for rock systems with a fluid phase containing one species (H_2O) soluble in silicate melt and one (CO_2) essentially insoluble in the melt. From Figure 4 and data on the relative proportions of phases in run products, we can also construct an isobaric section of the system andesite (Mount Hood)–H_2O (Fig. 8), in which H_2O is the only volatile species. Although Figures 4 and 8 show the same melting curves, their differences should be explicitly stated. The abscissa in Figure 4 is fluid composition, which is directly related to $f^{fl}_{H_2O}$ and therefore to $f^m_{H_2O}$ and to the H_2O content of the melt, but is related to bulk composition of

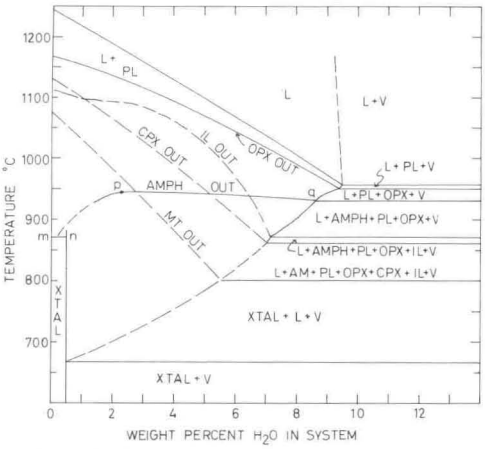

Figure 8. Melting relations in the system Mount Hood andesite–H_2O at 5 kb. Constructed curves are long dashed where run data are approximate.

the system only if the relative amounts of crystals and liquid are known. In Figure 8, on the other hand, the abscissa of the section is bulk composition of the system and gives no information on water content of the melt, except, of course, at the liquidus. Another difference is the extent of fluid-absent regions; in the system andesite–H_2O–CO_2, fluid exists even when the melt is H_2O undersaturated, whereas in the system andesite–H_2O, the melt can be H_2O undersaturated only in a fluid-absent region.

Solidus

In andesite–H_2O–CO_2, the solidus melting reaction is divariant, and its temperature, at any pressure, depends on the composition of the fluid (Fig. 4). Although Figure 4 shows the isobaric solidus as a smooth curve, in reality a break must occur at point b, where it intersects the divariant amphibole dehydration curve ab. The segment bf is a melting reaction not involving amphibole.

Point b is one point on a univariant curve which is formed by the loci of intersection of X_{H_2O} contours of the solidus and amphibole dehydration reactions. In the system andesite–H_2O, the same univariant reaction is the fluid-absent solidus, shown in P–T projection in Figure 1 and in T–X section in Figure 8 as line mn. Its temperature of 880° at 5 kb is the temperature of b in Figure 4. In andesite–H_2O (Fig. 8), beginning of melting occurs only by this reaction (at 880° at 5 kb) or by the fluid-present reaction (785° at 5 kb).

Liquidus Phases

As Yoder (1969) has noted, experimental melting relations of many andesite suites correspond to their petrography only if the magma is assumed to contain a small amount of H_2O. In Mount Hood andesite, 2 percent or more H_2O substantially reduces the melting interval between plagioclase and orthopyroxene (Fig. 8). In Paricutin andesite, 2 percent H_2O changes the liquidus phase to orthopyroxene, and 6 percent nearly places clinopyroxene on the liquidus (Fig. 4).

Amphibole Stability

Subsolidus stability of amphibole is governed by its dehydration reaction (curve ab in Fig. 4). In the system andesite–H_2O–CO_2, amphibole may not be a subsolidus phase when CO_2–rich fluids are present. In andesite–H_2O, on the other hand, amphibole is always a subsolidus phase (at 5 kb). It is often erroneously stated that the intersection of the H_2O–saturated solidus and amphibole-out curve (500 b for Mount Hood andesite; Fig. 1) is a limiting f_{H_2O} for crystallization of amphibole-bearing assemblages. Inasmuch as f_{H_2O} at b is 1,690 b, at any lower f_{H_2O} (at 5 kb) an amphibole-free rock will crystallize.

In the melting range, amphibole no longer breaks down by dehydration, but by one of several *melting* reactions. At H_2O–saturated conditions at 5 kb, amphibole in Mount Hood andesite melts at 930° (g, Fig. 4) to one or more (unknown) solid phases and to a liquid which must contain 9.5 percent H_2O. An incongruent reaction is postulated by analogy with basaltic melting relations (Holloway and Burnham, 1972). The melting temperature is considerably less than the temperature (c) of the metastable dehydration curve. At H_2O–undersaturated conditions, $f^m_{H_2O} < f^\circ_{H_2O}$, and the assemblage of amphibole, liquid, fluid, and other crystalline phases must melt at a higher temperature. The temperature increase in andesite (Fig. 4) at 5 kb is not large, but is more pronounced at higher pressure in basalt (Hill and Boettcher, 1970) and in pargasite–H_2O–CO_2 (Holloway, 1973). An equivalent effect is seen in andesite–H_2O (Fig. 8), as along pq $f^m_{H_2O} < f^\circ_{H_2O}$.

An isobaric temperature maximum of

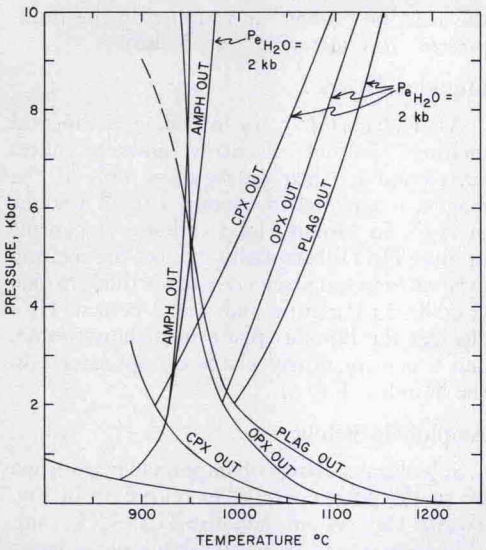

Figure 9. $P_{e_{H_2O}}$ **isobaric melting curves for Mount Hood andesite.**

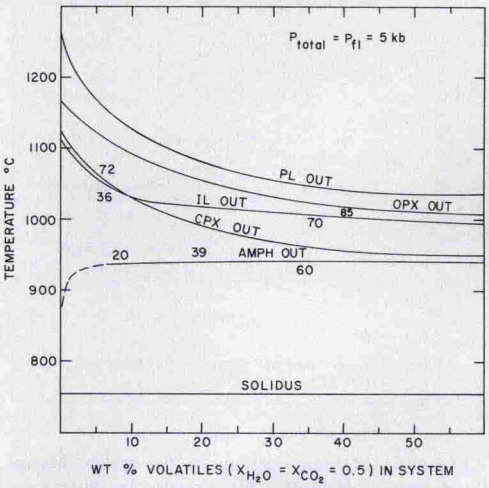

Figure 10. Relation of melting curves to percent volatiles (H_2O + CO_2) in the andesite–H_2O–CO_2 system at 5 kb.

stability is reached at d in Figure 4 and at p in Figure 8, points at which the melting curve breaks to intersect the solidus. Theoretical analysis of model systems (Eggler, in prep.) indicates that these maxima occur along *restricted univariant reactions*, at which a hydrous phase melts directly to solid phases and liquid; H_2O, other than that in the hydrous phase, is neither consumed nor released in the reaction. Along dg (Fig. 4), H_2O, in addition to that in the amphibole, must be supplied to saturate the melt, as in a "normal" melting reaction of an anhydrous silicate phase; along bd (Fig. 4) and np (Fig. 8), amphibole melts to a H_2O–poor liquid. Sufficient H_2O is evolved from the amphibole to saturate that liquid and to melt additional silicates in the process. The shape of curve bdg, only suggested by experimental runs, can be derived theoretically and has been dramatically confirmed by equivalent curves for pargasite–H_2O–CO_2 (Holloway, 1973).

$P_{e_{H_2O}}$ Isobars

$P_{e_{H_2O}}$ isobars have been constructed for Mount Hood andesite melt in Figure 9. They are constructed from T–X sections, such as in Figure 4. Because $X^{fl}{}_{H_2O}$ is assumed equal to $f_{H_2O}/f^{\circ}{}_{H_2O}$, $P_{e_{H_2O}}$ corresponding to any $X^{fl}{}_{H_2O}$ and, accordingly, f_{H_2O}, may be read from H_2O thermodynamic tables.

These isobars emphasize that the relative positions of melting curves determined at H_2O–saturated conditions ($P_{e_{H_2O}} = P_{total}$) are not the positions for the same $P_{e_{H_2O}}$ at other total pressures. Their positions are a function of temperature, total pressure, $P_{e_{H_2O}}$ (or, equivalently, $X^{fl}{}_{H_2O}$ or $f^{m}{}_{H_2O}$), and, in some cases, f_{O_2}. If the assumptions stated in this paper are correct, their position will not change whether H_2O is the only volatile species or whether H_2O + CO_2 are present.

Effect of Fluid-Phase Abundance

We have so far mentioned the composition of the fluid phase but not the amount of the phase present. In terms of phase relations, the amount of fluid present has no effect. Yet in assessing a crystallization history of a natural magma, the amount present at any time must be considered. Figure 10 illustrates the principle. A T–X section is constructed, in which X is the weight percent volatiles present, of composition 50 mole percent CO_2 – 50 mole percent H_2O, in a rock–H_2O–CO_2 system. The subsolidus fluid-phase composition is 50 percent H_2O, no matter how much (X) fluid is present. Above the solidus, H_2O must be partitioned between melt and fluid, so that, if very little fluid is present, that fluid may be very CO_2–rich.

The diagram shows that with an excess of fluid, the amount of fluid has no effect on the

melting curves. When less fluid is present, the position of a melting curve depends on the amount of fluid and on the amount of melt, for those factors determine the amount of H_2O in the melt.

In certain instances, this diagram may be applied to natural rocks. For instance, fluid inclusions effectively sample the subsolidus fluid phase, which on the diagram (and often in analyzed rocks) is 50 mole percent CO_2. If we could estimate the amount of fluid relative to rock, we could then deduce phase relations, melting temperatures, and fluid-phase composition in the hypersolidus region. Alternatively, inference of position of the melting curves from phenocryst assemblages could allow an estimate of the amount of fluid phase present.

Andesite Generation

Experiments and theory developed in this paper set limits on mechanisms for andesite generation by fractionation at pressures less than 10 kb, that is, in the crust and shallow upper mantle. Fractionation of basalt parents by plagioclase-pyroxene-oxide phase subtraction is unlikely because of the instability of oxide phases at the liquidus of andesite melt at reasonable geologic conditions. Fractionation by subtraction of amphibole is also unlikely, because in two separate andesites studied, amphibole is not stable at the liquidus below 8 kb and is not stable at the liquidus in H_2O–undersaturated melts at pressures to 10 kb. (The effect of other volatiles, particularly fluorine, has not been investigated and may be large.)

Partial melting at greater depths in the upper mantle, either of subducted basaltic oceanic floor or of peridotite, is a more reasonable mechanism. Such melts must be hydrous, both to produce requisite andesitic compositions (Kushiro, 1972), and because andesite melts can be shown to contain small but significant amounts of H_2O (Eggler, 1972a). The water content of initial melts should be estimated, for it provides one more clue to the nature of the upper mantle.

REFERENCES CITED

Allen, J. C., and Boettcher, A. L., 1971, The stability of amphiboles in basalts and andesites at high pressures: Geol. Soc. America, Abs. with Programs (Ann. Mtg.), v. 3, no. 7, p. 490.

Anderson, A. T., 1968, The oxygen fugacity of alkaline basalt and related magmas, Tristan da Cunha: Am. Jour. Sci., v. 266, p. 704–727.

Boettcher, A. L., and Wyllie, P. J., 1968, Melting of granite with excess water to 30 kilobars pressure: Jour. Geology, v. 76, p. 235–244.

Buddington, A. F., and Lindsley, D. H., 1964, Iron-titanium oxide minerals and synthetic equivalents: Jour. Petrology, v. 5, p. 310–357.

Burnham, C. W., 1967, Hydrothermal fluids at the magmatic stage, *in* Barnes, H. L., ed., Geochemistry of hydrothermal ore deposits: New York, Holt, Rinehart and Winston, p. 34–76.

Burnham, C. W., and Davis, N. F., 1971, The role of H_2O in silicate melts I. P-V-T relations in the system $NaAlSi_3O_8$–H_2O to 10 kilobars and 1,000° C: Am. Jour. Sci., v. 270, p. 54–79.

Burnham, C. W., Holloway, J. R., and Davis, N. F., 1969, The specific volume of water in the range 1,000–8,900 bars, 20°–900° C: Am. Jour. Sci., v. 267–A (Schairer volume), p. 70–95.

Carmichael, I.S.E., 1967, The iron-titanium oxides of salic volcanic rocks and their associated ferromagnesian silicates: Contr. Mineralogy and Petrology, v. 14, p. 36–64.

Carmichael, I.S.E., and Nicholls, J., 1967, Iron-titanium oxides and oxygen fugacities in volcanic rocks: Jour. Geophys. Research, v. 72, p. 4665–4687.

Darken, L. S., and Gurry, R. W., 1945, The system iron-oxygen. I. The Wustite field and related equilibria: Jour. Am. Chemical Soc., v. 67, p. 1398–1412.

Dodge, F.C.W., Smith, V. C., and Mays, R. E., 1969, Biotites from granitic rocks of the central Sierra Nevada batholith, California: Jour. Petrology, v. 10, p. 250–271.

Eggler, D. H., 1971, Model for calcalkaline fractional crystallization under water-saturated and undersaturated conditions: A portion of the system $NaAlSi_3O_8$–$CaAl_2Si_2O_8$–SiO_2–MgO–FeO–Fe_2O_3–H_2O–CO_2: Geol. Soc. America, Abs. with Programs (Ann. Mtg.), v. 3, no. 7, p. 553–554.

—— 1972a, Water-saturated and undersaturated melting relations in a Paricutin andesite and an estimate of water content in the natural magma: Contr. Mineralogy and Petrology, v. 34, p. 261–271.

—— 1972b, Amphibole stability in H_2O–undersaturated calc-alkaline melts: Earth and Planetary Sci. Letters, v. 15, p. 28–34.

Eggler, D. H., and Osborn, E. F., 1969, Experimental data for the system MgO–FeO–Fe_2O_3–$NaAlSi_3O_8$–$CaAl_2Si_2O_8$–SiO_2 and their petrologic application: Am. Geophys. Union Trans., v. 50, p. 337.

Fudali, R. F., 1965, Oxygen fugacities of basaltic and andesitic magma: Geochim. et Cosmochim. Acta, v. 29, p. 1063–1075.

Green, T. H., and Ringwood, A. E., 1966, Origin of the calcalkaline igneous rock suite: Earth and Planetary Sci. Letters, v. 1, p. 307–316.

—— 1968, Genesis of the calc-alkaline igneous rock suite: Contr. Mineralogy and Petrology, v. 18, p. 105–162.

Hamilton, D. L., and Anderson, G. M., 1967, Effects of water and oxygen pressures on the crystallization of basaltic magmas, *in* Hess, H. H., and Poldervaart, A., eds., Basalts: New York, Interscience Pub., v. 1, p. 445–482.

Hamilton, D. L., Burnham, C. W., and Osborn, E. F., 1964, The solubility of water and effects of oxygen fugacity and water content on crystallization in mafic magmas: Jour. Petrology, v. 5, p. 21–39.

Hill, R.E.T., and Boettcher, A. L., 1970, Water in the earth's mantle: Melting curves of basalt-water and basalt–water–carbon dioxide: Science, v. 167, p. 980–982.

Holloway, J. R., 1973, The system pargasite–H_2O–CO_2: A model for melting of a hydrous mineral with a mixed-volatile fluid. I. Experimental results to 8 kb: Geochim. et Cosmochim. Acta, v. 37, p. 651–666.

Holloway, J. R., and Burnham, C. W., 1972, Melting relations of basalt with equilibrium water pressure less than total pressure: Jour. Petrology, v. 13, p. 1–29.

Holloway, J. R., Burnham, C. W., and Millhollen, G. L., 1968, Generation of H_2O–CO_2 mixtures for use in hydrothermal experimentation: Jour. Geophys. Research, v. 73, p. 6598–6600.

Holloway, J. R., Eggler, D. H., and Davis, N. F., 1971, An analytical expression for calculating the fugacity and free energy of H_2O to 10,000 bars and 1,300°C: Geol. Soc. America Bull., v. 82, p. 2639–2642.

Kushiro, I., 1972, Effect of water on the compositions of magmas formed at high pressures: Jour. Petrology, v. 13, p. 311–334.

Millhollen, G. L., Wyllie, P. J., and Burnham, C. W., 1971, Melting relations of $NaAlSi_3O_8$ to 30 kb in the presence of H_2O:CO_2 = 50:50 vapor: Am. Jour. Sci., v. 271, p. 473–480.

Mueller, R. F., 1969, Hydration, oxidation, and the origin of the calc-alkali series: NASA Tech. Note D-5400, 27 p.

—— 1971, Oxidative capacity of magmatic components: Am. Jour. Sci., v. 270, p. 236–243.

Osborn, E. F., 1959, Role of oxygen pressure in the crystallization and differentiation of basaltic magma: Am. Jour. Sci., v. 257, p. 609–647.

—— 1969, The complementariness of orogenic andesite and alpine peridotite: Geochim. et Cosmochim. Acta, v. 33, p. 307–324.

Presnall, D. C., 1966, The join forsterite–diopside–iron oxide and its bearing on the crystallization of basaltic and ultramafic magmas: Am. Jour. Sci., v. 264, p. 753–809.

Robertson, J. K., and Wyllie, P. J., 1971, Rock-water systems, with special reference to the water-deficient region: Am. Jour. Sci., v. 271, p. 252–277.

Robie, R. A., and Waldbaum, D. R., 1968, Thermodynamic properties of minerals and related substances at 298.15°K (25°C) and one atmosphere (1.013 bars) pressure and at higher temperatures: U.S. Geol. Survey Bull. 1259, 259 p.

Roeder, P. L., and Osborn, E. F., 1966, Experimental data for the system MgO–FeO–Fe_2O_3–$CaAl_2Si_2O_8$–SiO_2 and their petrologic implications: Am. Jour. Sci., v. 264, p. 428–480.

Shaw, H. R., 1967, Hydrogen osmosis in hydrothermal experiments, *in* Abelson, P. H., ed., Researches in geochemistry, v. 2: New York, John Wiley & Sons, Inc., p. 521–541.

Shaw, H. R., and Wones, D. R., 1964, Fugacity coefficients for hydrogen gas between 0° and 1,000°C, for pressures to 3,000 atm: Am. Jour. Sci., v. 262, p. 918–929.

Williams, R. J., 1971, Reaction constants in the system Fe–MgO–SiO_2–O_2 at 1 atm between 900°C and 1,300°C: Experimental results: Am. Jour. Sci., v. 270, p. 334–360.

Wise, W. S., 1969, Geology and petrology of the Mount Hood area: A study of High Cascade volcanism: Geol. Soc. America Bull., v. 80, p. 969–1006.

Wyllie, P. J., and Tuttle, O. F., 1959, Effect of carbon dioxide on the melting of granite and feldspars: Am. Jour. Sci., v. 257, p. 648–655.

Yoder, H. S., Jr., 1969, Calc-alkaline andesites: Experimental data bearing on the origin of their assumed characteristics: Proceedings of the Andesite Conference: Oregon Dept. Geology and Mineral Industries Bull. 65, p. 77–89.

Yoder, H. S., Jr., and Tilley, C. E., 1962, Origin of basalt magmas: An experimental study of natural and synthetic rock systems: Jour. Petrology, v. 3, p. 342–532.

Zen, E-An, 1966, Construction of pressure-temperature diagrams for multi-component systems after the method of Schreinemakers—A geometric approach: U.S. Geol. Survey Bull. 1225, 56 p.

Manuscript Received by the Society July 31, 1972

PRINTED IN U.S.A.